Dual-mode coupled-resonator integrated optical filters

C. Alonso-Ramos, F. Morichetti, A. Ortega-Moñux, I. Molina-Fernández, M. J. Strain, A. Melloni

***Abstract*—A photonic integrated architecture realizing the concept of coupled-resonator dual-mode optical filters is presented. The proposed structure consists of a chain of directly coupled microring resonators with a partial reflector embedded in the last resonator. The contradirectional coupling induced by the reflector makes the effective order of the filter double with respect to the number of coupled resonators. Since the counterpropagating modes share the same physical cavity, the resonant frequencies are intrinsically aligned, the sensitivity of the filter to fabrication tolerances is reduced and the control of the structure is eased with respect to coupled resonator filters of the same order. Second- and fourth-order dual-mode filters made of microring resonators loaded with a Bragg grating are experimentally demonstrated on a silicon-on-insulator (SOI) photonic platform.**

***Index Terms*—Integrated optics, Filters, Resonators, Bragg reflector.**

I. Introduction

MICRORING resonators are widely used as building blocks for the implementation of integrated photonic devices and circuits such as fixed and tunable filters, add/drop multiplexers, delay lines, modulators and sensors [1]. In many of these applications the spectral properties of single-ring devices are often unsatisfactory and higher-order structures, comprising several coupled resonators, are required to achieve transfer functions with a high extinction ratio and sharp band-edge transitions [2]. Extremely compact coupled-resonator devices with a large bandwidth and free spectral range (FSR) can be realized by using high-index-contrast technologies, like silicon-on-insulator (SOI) photonic platforms. However, these technologies suffer from a high sensitivity to fabrication tolerances, leading to a random spectral spreading of the resonant frequencies of the resonators. Power-consuming tuning actuators and/or post-fabrication trimming techniques are thus required to set the resonance frequencies to the proper spectral position and restore the desired device functionality [3-5].

In this letter, we propose a novel coupled-resonator filter architecture that implements higher-order responses exhibiting an intrinsically high robustness against fabrication tolerances. We exploit the concept of dual-mode filters that is widely used in the microwave field [6] and that has been recently transferred to photonic integrated platforms to engineer device reflectivity [7], [8]. Single-cavity dual-mode photonic filters have been proposed that use a partial reflector inside a microring resonator to implement a second-order response [9]. Higher-order dual-mode filters have also been theoretically proposed that use serial and parallel reflection topologies [10].

One of the main advantages of dual-mode filters is that the effective order of the filter can be higher than the number of coupled cavities. The dual-mode photonic filter proposed here exploits the contradirectional coupling induced by a partial reflector embedded inside a chain of coupled racetrack resonators in such a way that the resulting filter order is twice the total number of coupled resonators. Since the forward- and backward-propagating modes share the same physical cavity, their resonant frequencies are inherently aligned [11], [12], so that both the fabrication process and the control of the circuit are eased. Following this approach, we experimentally demonstrate a fourth-order dual-mode photonic integrated filter fabricated on a SOI platform, consisting of two coupled racetrack resonators with a single embedded Bragg grating used as a partial reflector.

II. Dual-mode coupled-resonator filters

In order to illustrate the concept of dual-mode coupled-resonator filters, the model of a dual-mode single-resonator filter needs to be briefly described. Dual-mode behavior can be induced by inserting a partial reflector inside a microring resonator [7-9], as schematically shown in Fig. 1(a). The resonator, with a round-trip geometric length L_r, is coupled to a bus waveguide by a directional coupler with field coupling coefficient jt_c (j unit is omitted in all the figures for the sake of clarity). The field reflection and transmission coefficients of the partial reflector are jr_g and t_g, respectively ($|r_g|^2 + |t_g|^2 = 1$). The contradirectional mode coupling induced by the reflector makes the single-ring filter behave like the equivalent circuit shown in Fig. 1(b), which is made of two identical coupled rings connected to an input- and an output-bus waveguide. The coupling coefficients between the rings and the bus waveguides are both equal to jt_c, whereas the coupling between the two rings is provided by r_g. The field reflection response R_x of the dual-mode filter, corresponding to the drop-port of the two-ring equivalent circuit, is given by

$$R_x(z) = \frac{r_g t_c^2 z^{-1}}{r_c^2 z^{-2} - 2r_c t_g z^{-1} + 1}, \tag{1}$$

where r_c is the bar-port coupling coefficient of the directional coupler, $z^{-1} = \gamma \exp(-j\beta L_r)$, γ is the round-trip loss

C. Alonso-Ramos, A. Ortega-Moñux and I. Molina-Fernández are with the Departamento Ingeniería de Comunicaciones, ETSI Telecomunicación, Universidad de Málaga 29071 Málaga, Spain e-mail: caar@ic.uma.es.

F. Morichetti and A. Melloni are with the Dipartimento di Elettronica, Informazione e Bioingegneria - Politecnico di Milano, via Ponzio 34/5, 20133 Milano, Italy.

M. J. Strain is with the Institute of Photonics, The University of Strathclyde, Glasgow G4 0NW

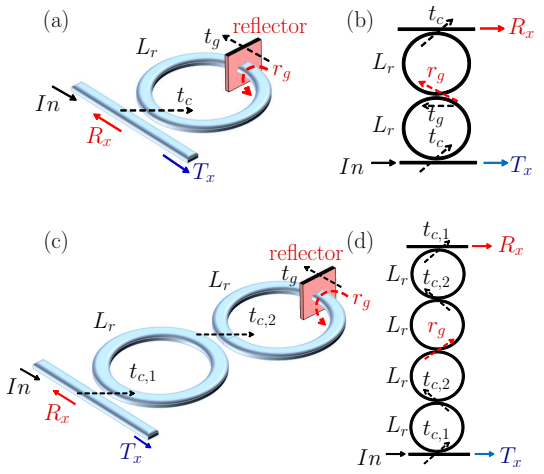

Fig. 1. (a) Schematic and (b) equivalent circuit of a single-resonator dual-mode filter consisting of a ring resonator loaded with a partial reflector. (c) Schematic and (d) equivalent circuit of the proposed dual-mode coupled-resonator filter implementing a fourth-order passband filter.

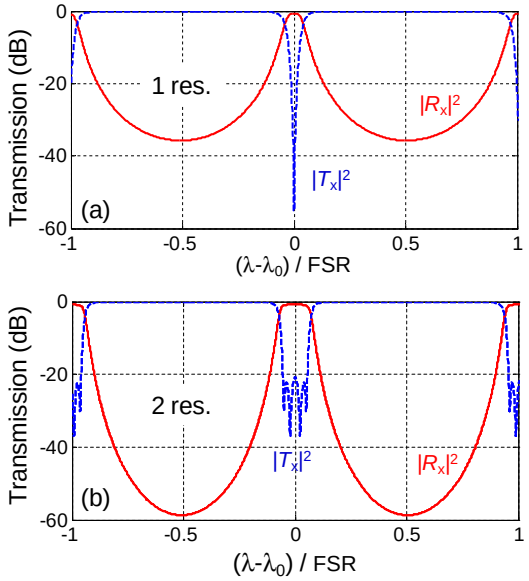

Fig. 2. Simulated intensity transmission $|T_x|^2$ (blue dashed lines) and reflection $|R_x|^2$ (red solid lines) of (a) a single-ring ($|t_c|^2 = 0.3$, $|r_g|^2 = 0.031$) and (b) a two-ring dual-mode filter ($|t_{c,1}|^2 = 0.53$, $|t_{c,2}|^2 = 0.096$, and $|r_g|^2 = 0.058$).

coefficient, and β is the propagation constant of the optical mode. Likewise, the transmission response T_x, corresponding to the through-port of the equivalent circuit, reads

$$T_x(z) = \frac{r_c z^{-2} - t_g\left(1 + r_c^2\right) z^{-1} + r_c}{r_c^2 z^{-2} - 2 r_c t_g z^{-1} + 1}. \tag{2}$$

The two poles in the R_x and T_x transfer functions indicate a second-order behavior for the filter. If $r_c < \gamma$, that is if the all-pass filter hosting the partial reflector has a maximum phase response [13], a critical value exists

$$t_{g,cr} = \frac{r_c(1+\gamma^2)}{\gamma(1+r_c^2)}, \tag{3}$$

for which T_x vanishes and the input signal is totally reflected (R_x =1). In the case of lossless filters (γ = 1), eq. (3) provides also maximally flat passband, since both zeros of eq. (2) lie onto the unitary circle.

It should be noted that eqs. (1) and (2) recall the expressions describing the effect of polarization rotation inside a ring resonator [14]. Indeed in both cases a coupling between two modes sharing the same physical cavity occurs. The main difference with respect to the case of polarization rotation is that the counterpropagating modes are here inherently phase matched because they have the same propagation constant β.

The single-ring dual-mode scheme is here extended to higher-order filters with an arbitrary number of coupled resonators. For example, Fig. 1(c) shows a dual-mode filter comprising two directly-coupled microrings with a partial reflector embedded in the second resonator, and realizing the fourth-order filter shown in Fig. 1(d). The field coupling coefficients $jt_{c,1}$ of the equivalent circuit, connecting the bus waveguides to the external rings, are those of the original directional couplers, as well as the coupling $jt_{c,2}$ between the first and the second rings at both sides of the filter. Similarly to the single ring structure of Fig. 1(a), the central coupling coefficient jr_g of the equivalent circuit is provided by the reflection coefficient of the partial reflector. Following this approach, filters with arbitrarily high orders can be designed, where only one partial reflector needs to be inserted in the last resonator of the chain. Within the reflection bandwidth of the reflector, the reflection R_x and the transmission T_x of the dual-mode filter coincide respectively with the drop-port and through-port response of the coupled-resonator equivalent filter. Note that the In- and R_x-port share the same waveguide, and an optical circulator is required to retrieve the signal from the R_x-port. Standard synthesis techniques for coupled-resonator filters directly apply to the equivalent circuit and can be effectively exploited for the design of the proposed dual-mode filters [17]. Further, it should be noted that any contribution given by the partial reflector to the round-trip phase of the ring is shared by the two counter-propagating modes, thereby not affecting the resonance alignment mechanism of the dual-mode filter.

Figure 2 shows the simulated spectra of the intensity transmission $|T_x|^2$ (blue dashed lines) and reflection $|R_x|^2$ (red solid lines) across two FSRs of a single-ring (a) and of a two-ring (b) dual-mode filter. The 3-dB bandwidth of the filters is about 0.1 FSR, while the round-trip loss of each resonator, taking into account both propagation loss in the bent waveguide and the excess loss of the directional coupler, is 0.15 dB/turn. The $|T_x|^2$ response of the single-ring filter (second-order response), working at the critical coupling condition, given by eq. (3), exhibits an in-band transmission zero with a width of 0.027 FSR at -20 dB rejection, while the $|R_x|^2$ spectrum has a maximum off-band rejection of more than 30 dB. As shown in Fig. 2(b), the spectral properties of the filter can be improved by using a two-ring coupled-resonator structure, according to the scheme of Fig. 1(c). This architecture implements a fourth-order filter with a 20-dB-rejection bandwidth as large as 0.11 FSR in the T_x response, and a maximum off-band rejection higher than 55 dB in the $|R_x|^2$ response. Further improvements are expected when

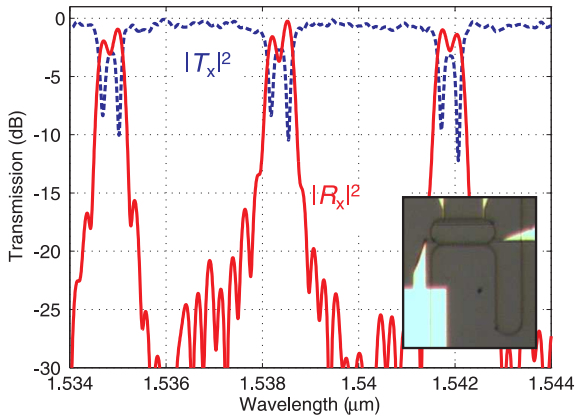

Fig. 3. Normalized measured transmission $|T_x|^2$ (blue dashed curve) and reflection $|R_x|^2$ (red solid curve) of a single-resonator dual-mode filter made of an SOI racetrack loaded with a Bragg grating: spectral response over a wavelength range of 10 nm centered around 1539 nm.

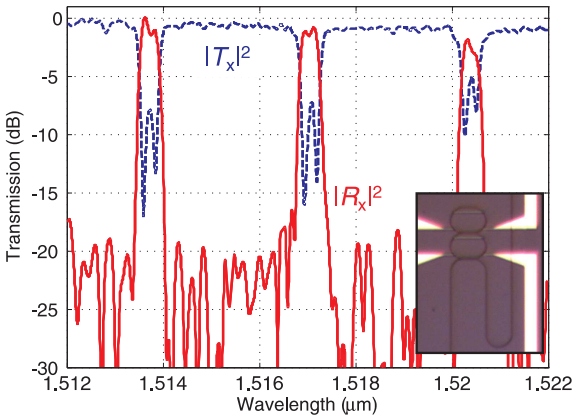

Fig. 4. Normalized measured transmission $|T_x|^2$ (blue dashed curve) and reflection $|R_x|^2$ (red solid curve) of proposed SOI two-resonator dual-mode filter: spectral response over a wavelength range of 10 nm centered around 1517 nm.

more than two rings are cascaded [17].

III. Experimental Results

Single-resonator and coupled-resonators dual-mode photonic integrated filters were fabricated on a conventional 220 nm SOI platform using hydrogen silsesquioxane (HSQ) electron-beam-resist-based technology [15]. The optical waveguide has a rectangular silicon core with a width w = 480 nm and is buried under a 1 μm thick silica cladding. The racetrack resonators have a bending radius of 20 μm and a geometric length L_r = 158 μm, resulting in a FSR of 450 GHz. In the coupled-resonator structures, the coupling coefficients of the directional couplers are optimized by changing the gap distance between the straight waveguide sections, whose length is fixed to 16 μm. The partial reflector consists of a uniform Bragg grating obtained by periodically varying the width of the waveguide. The round-trip loss of the resonators (estimated at wavelengths outside the reflection bandwidth of the grating) is about 0.15 dB/turn.

Light generated by a tunable laser is injected to and collected from the chip using tapered lensed fibers. A polarization-controller is used to set a transverse electric (TE) polarization at the chip input with more than 30 dB extinction ratio. The reflection spectrum $|R_x|^2$ of the filter is measured by extracting the reflected light through an optical circulator placed before the launch fiber. The measured spectra are processed with the minimum phase technique [16] to remove the Fabry-Pérot ripples produced by facet reflections.

Fig. 3 shows the measured intensity transmission $|T_x|^2$ (blue dashed line) and reflection $|R_x|^2$ (red solid line) of a single-resonator dual-mode filter with $|t_c|^2 = 0.3$ and a Bragg grating peak reflectivity $|r_g|^2 = 0.1$. The gap distance between the waveguides in the directional coupler of the resonator is 230 nm. The Bragg grating has 14 periods of a rectangular profile with 10 nm depth at each side, that is w locally changes from 490 nm to 470 nm around the nominal width of the unperturbed waveguide. The grating period Λ = 320 nm is designed to set the Bragg wavelength around 1550 nm with a a 3-dB bandwidth of 57 nm. The reflection spectrum $|R_x|^2$ has a bandwidth of about 75 GHz, a good off-band rejection ($>$ 20 dB) and a sharp transition at the edges of the passing bands (about 0.5 dB/GHz). The 3-dB ripple in the passband is mainly due to the overcoupling regime of the filter, which is also responsible for the limited in-band isolation in the transmission spectrum. Comparisons with numerical simulations show that the Bragg grating scattering loss (estimated below 0.5 dB) does not impact significantly the device performance. Since the two counterpropagating modes share the same physical cavity, the resonance frequencies of the filter are intrinsically aligned, independently of any fabrication tolerances and environmental fluctuations, avoiding the need for an active tuning of the spectral response.

Fig. 4 shows the measured spectral response of a fabricated SOI coupled-resonator dual-mode filter made of two racetrack resonators loaded with a Bragg grating. The reflection spectrum $|R_x|^2$ (red solid line) has a bandwidth of about 50 GHz with an increased slope of the band-edge transitions (1.3 dB/GHz) compared to the single-resonator filter of Fig. 3. The level of the off-band reflected signal is addressable mainly to the roughness-induced backscattering of the bus waveguide [18], limiting the actual filter isolation to about 20 dB. A maximally flat reflection spectrum with less than 1.5 dB in-band ripple is achieved by using directional couplers with $|t_{c,1}|^2 = 0.57$, $|t_{c,2}|^2 = 0.12$ and a Bragg grating with a peak reflectivity $|r_g|^2 = 0.075$. The gap distance between the waveguides of the directional couplers is 194 nm ($t_{c,1}$) and 300 nm ($t_{c,2}$). The Bragg grating has a sinusoidal profile and counts 24 periods with a 5 nm peak-to-peak depth at each side ($475 < w < 485$) and a period Λ = 312 nm, resulting in a Bragg wavelength of about 1515 nm with a 3dB bandwidth of 32 nm. Around the Bragg wavelength the transmission spectrum of the filter ($|T_x|^2$, blue dashed line) exhibits a deep wide notch with an in-band extinction of about 8 dB. It should be noted that a single thermo-optic metal actuator realized onto the first resonator of the filter was used to align the resonances of the two resonators, thus achieving a very simple and power effective ($<$ 10 mW) tuning of the fourth-order filter.

A further confirmation of the dual-mode behavior of the

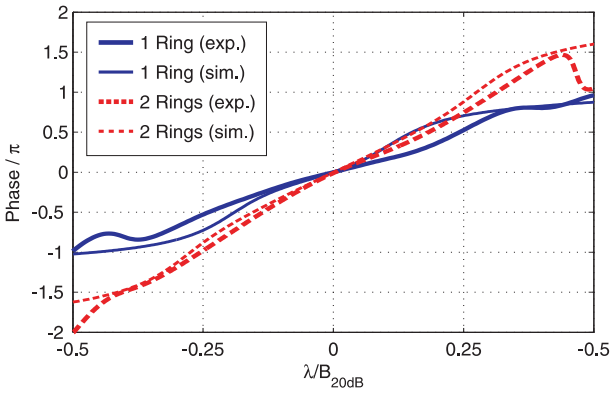

Fig. 5. Measured (thick curves) and simulated (thin curves) phase-shift of the transfer function R_x across the reflection band of the single-resonator filter of Fig. 3 (blue solid) and the two-resonator filter of Fig. 4 (red dashed).

proposed filters is provided by a phase analysis of the spectral response. Let us remind that the drop-port transmission of a conventional coupled-resonator filter with N cascaded resonators exhibit a $N\pi$ phase shift across the passband [13]. If it is true that the approach proposed in our work doubles the order of the filter, then the realized dual-mode architectures should exhibit a $2N\pi$ phase shift across the reflection band. The phase of the reflection transfer function R_x was measured by using a coherent optical frequency-domain reflectometer [18]. Figure 5 shows the measured (thick curves) and simulated (thin curves) phase shift of the single-resonator (blue solid) and the two-resonator (red dashed) dual-mode filters. The phase shift is evaluated within the reflection bandwidth B_{20dB}, defined at 20 dB attenuation from the peak reflection. The single-resonator filter exhibits a 2π phase shift, while the two-resonator filter shows a 4π phase shift, proving that the proposed structures effectively implement a $2N$-th order filter response with only N resonators.

IV. Conclusion

Contra-directional coupling in coupled-resonator structures has been exploited to experimentally demonstrate the concept of high-order dual-mode photonic filters. Not only the proposed approach enables to double the filter order with respect to the number of coupled resonators, but since the forward- and backward-propagating modes resonate in the same physical cavity, their resonant frequencies are intrinsically aligned. This means that, for a given filter order, the sensitivity to fabrication tolerances is reduced as well as the number of active controls of the resonators, thereby resulting in an easier and power-efficient tuning of the filter. Using this scheme we have implemented a fourth-order filter made of only two racetrack resonators, showing also that the proposed approach is straightforwardly scalable to higher-order filters. The concept of dual-mode filters could be further generalized by realizing filters based also on the coupling between orthogonally polarized modes [19] and higher-order modes, opening new perspectives for the implementation of advanced filtering functions in photonic integrated circuits.

Acknowledgment

This work was partially supported by the Italian PRIN 2009 project Shared Access Platform to Photonic Integrated Resources (SAPPHIRE) and by the FP7-ICT European FET Project BBOI. The Authors gratefully acknowledge M. Sorel and the James Watt Nanofabrication Centre (JWNC) staff at Glasgow University for the fabrication of the devices, and S. Grillanda for the support in the optical characterization of the devices.

References

[1] W. Bogaerts, P. De Heyn, T. Van Vaerenbergh, K. De Vos, S. Kumar Selvaraja, T. Claes, P. Dumon, P. Bienstman, D. Van Thourhout, and R. Baets, "Silicon microring resonators," Laser & Photon. Rev., vol. 6, no. 1, pp. 47–73, Jan, 2012.

[2] F. Xia, M. Rooks, L. Sekaric, and Y. Vlasov, "Ultra-compact high order ring resonator filters using submicron silicon photonic wires for on-chip optical interconnects," Opt. Express, vol. 15, no. 19, pp. 11934–11941, Sep 2007.

[3] Y. Shen, I. Divliansky, D. Basov, and S. Mookherjea, "Electric-field-driven nano-oxidation trimming of silicon microrings and interferometers," Opt. Lett., vol. 36, no. 14, pp. 2668–2670, Jul 2011.

[4] A. Canciamilla, F. Morichetti, S. Grillanda, P. Velha, M. Sorel, V. Singh, A. Agarwal, L. Kimerling, and A. Melloni, "Photo-induced trimming of chalcogenide-assisted silicon waveguides," Opt. Express, vol. 20, no. 14, pp. 15807–15817, Jul. 2012.

[5] J. R. Ong, R. Kumar, and S. Mookherjea, "Ultra-high-contrast and tunable-bandwidth filter using cascaded high-order silicon microring filters," IEEE Photon. Technol. Lett., vol. 25, no. 16, pp. 1543–1546, Aug. 2013.

[6] A. E. Atia and A. E. Williams, "Narrow bandpass waveguide filters," IEEE Trans. Microwave Theory Tech., vol. 20, no. 4, pp. 258–265, Apr. 1972.

[7] Y. M. Kang, A. Arbabi, and L. L. Goddard, "Engineering the spectral reflectance of microring resonators with integrated reflective elements," Opt. Express, vol. 18, no. 16. pp. 16813–16825, Aug. 2010.

[8] G. T. Paloczi, J. Scheuer, and A. Yariv, "Compact Microring-Based Wavelength-Selective Inline Optical Reflector," IEEE Photon. Technol. Lett., vol. 17, no. 2, pp. 390–392, Feb. 2005.

[9] B. E. Little, S. T. Chu, and H. A. Haus, "Second-order filtering and sensing with partially coupled traveling waves in a single resonator," Opt. Lett., vol. 23, no. 20, pp. 1570–1572, Oct. 1998.

[10] V. Van, "Dual-Mode Microring Reflection Filters," J. Lightw. Techn., vol. 25, no. 10, pp. 3142–3150, Oct. 2007.

[11] J. Čtyroký, I. Richter, and M. Šiňor, "Dual resonance in a waveguide-coupled ring microresonator," Opt. Quantum Electron., vol. 38, no. 9, pp. 781-797, Jul. 2006.

[12] Z. Zhang, M. Dainese, L. Wosinski, and M. Qiu, "Resonance-splitting and enhanced notch depth in SOI ring resonators with mutual mode coupling," Opt. Express, vol. 16, no. 7, pp. 4621–4630, Mar. 2008.

[13] C. K. Madsen and J. H. Zhao, Optical Filter Design and Analysis: A Signal Processing Approach, Wiley Series in Microwave and Optical Engineering (Wiley, 1999)

[14] A. Melloni, F. Morichetti, and M. Marinelli, "Polarization conversion in ring resonator phase shifters," Opt. Lett., vol. 29, no. 23, pp. 2785–2787, Dec. 2004.

[15] M. Gnan, S. Thorns, D. S. Macintyre, R. M. De La Rue and M. Sorel, "Fabrication of low-loss photonic wires in silicon-on-insulator using hydrogen silsesquioxane electron-beam resist," Electr. Lett., vol. 44, no. 2, pp. 115–116, Jan. 2008.

[16] R. Halir, I. Molina-Fernández, J.G. Wangüemert-Pérez, A. Ortega-Moñux, J. de-Oliva-Rubio, and P. Chenben, "Characterization of integrated photonic devices with minimum phase technique," Opt. Express, vol. 17, no. 10, pp. 8349–8361, May. 2009.

[17] A. Melloni and M. Martinelli, "Synthesis of direct-coupled-resonators bandpass filters for WDM systems," J. Lightw. Techn., vol. 20, no. 2, pp. 296–303, Feb. 2002.

[18] F. Morichetti, A. Canciamilla, C. Ferrari, M. Torregiani, A. Melloni, and M. Martinelli, "Roughness induced backscattering in optical silicon waveguides," Phys. Rev. Lett., vol. 104, pp. 033902-1–033902-4, Jan. 2010.

[19] F. Morichetti and A. Melloni, "Polarization converters based on ring-resonator phase-shifters," IEEE Phot. Techn. Lett., vol.18, no.8, pp. 923-925, Apr. 2006.